ADVANCED OPTICAL MATERIALS
www.advopticalmat.de

# Photo-Controlled Reversible Multicolor Room-Temperature Phosphorescent Solid Supramolecular Pseudopolyrotaxane

*Yi Zhang, Cong Zhang, Yong Chen, Jie Yu, Lei Chen, Hui Zhang, Xiufang Xu, and Yu Liu**

**The photoreversible switch persistent room-temperature phosphorescent (p-RTP) system is attractive but challenging in the field of smart luminescent materials. In particular, those p-RTPs with the excitation-wavelength-responsive and time-dependent multicolor emission are very important but underexplored. Herein an excitation-wavelength-responsive and time-dependent multicolor p-RTP emission pseudopolyrotaxanes supramolecular system based on host–guest interaction between $\alpha$-cyclodextrin ($\alpha$-CD) and two luminophores (benzene and naphthalene) modified polyethylene glycol (PEG) derivatives is reported. The excitation-wavelength-responsive and time-dependent multicolor afterglows of the supramolecular system are derived from the diverse p-RTP emission species with different lifetimes. More importantly, the p-RTP can be reversibly adjusted by photoisomerization of diarylethylene (DAE), that is, it could be erased under ultraviolet light and recovered under visible-light for several cycles. Taking advantage of the reversible photoencryption property, this intelligent luminescence supramolecular system has broad application prospects in information storage and treatment.**

## 1. Introduction

Room-temperature phosphorescence (RTP) materials have received extensive attention in the fields of chemical sensing,[1] information anti-counterfeiting,[2] and bioimaging.[3] Among them, supramolecular systems with phosphorescent emission have become research hotspots because the non-covalent interactions have a significant impact on the luminescent properties of the materials.[4] Compared with several methods that have been reported to achieve persistent room-temperature phosphorescent (p-RTP), such as reasonable molecular design,[5] crystallization,[6] or embedding phosphors into appropriate matrices,[7] supramolecular non-covalent interaction can enhance room-temperature phosphorescence by an efficient and convenient way with several advantages including 1) the encapsulation of the macrocyclic hydrophobic cavity can not only promote the intersystem crossing (ISC) of the phosphorescent guest but also limit the molecular motion to promote RTP under room temperature;[8] 2) the ordered structure or abundant hydrogen bonds of supramolecular assemblies provide a rigid microenvironment that can stabilize the triplet state and shield quenchers (such as oxygen, $H_2O$) to inhibit the non-radiative transitions to enhance RTP emission;[9] 3) the preparation process of supramolecular systems is gentle and does not involve complicated molecular design and synthesis.[10] For example, Ma and co-workers reported a series of effective phosphorescent compounds by modifying phosphors to cyclodextrin(CD), wherein the hydrogen bond interaction between CDs can effectively inhibit non-radiation transition and promote RTP emission.[4b] We reported that the encapsulation of cucurbit[6]uril can promote ISC and inhibit molecular motions of the guest phenylmethylpyridinium to achieve p-RTP with a 2.62 s ultralong lifetime.[11] Recently, we also constructed supramolecular pins with ultrahigh fluorescence quantum yield. This property is achieved by the molecular folding bonding of cucurbit[8]uril and the bridged phenylpyridinium salt, which strictly restricts the molecular vibration of the chromophore.[12]

Stimulus-response RTP supramolecular materials have been widely employed in the field of high-density recording,[13] multicolor display[14] and information encryption.[15] So far, this stimulus-responsive material is mainly constructed by regulating the noncovalent forces, e.g., hydrogen bonds,[2b,16] host–guest interactions,[17] in the system. Zhao et al. reported a series of multicolor RTP polymers with humidity response due to the influence of water molecules on hydrogen bonds in the system.[18] Tian et al. reported a supramolecular hydrogel that utilizing the photoisomerization of azobenzene to control the host–guest interaction between CD and phosphors group to achieve photo-response RTP.[19] However, these studies mainly focus on the stimulus-responsive regulation of relatively short-lived phosphorescence, while the regulation of long-lived RTP with afterglow is still rare. Therefore, we construct the photoreversible multicolor p-RTP supramolecular pseudopolyrotaxane systems by efficient energy transfer between the phosphorescent compound and the photochromic diarylethene (DAE). The supramolecular system is composed of DAE and pseudopolyrotaxane by $\alpha$-cyclodextrin ($\alpha$-CD) and polyethylene glycol

Y. Zhang, C. Zhang, Y. Chen, J. Yu, L. Chen, H. Zhang, X. Xu, Y. Liu
College of Chemistry
State Key Laboratory of Elemento-Organic Chemistry
Nankai University
Tianjin 300071, P. R. China
E-mail: yuliu@nankai.edu.cn

The ORCID identification number(s) for the author(s) of this article can be found under https://doi.org/10.1002/adom.202102169.

DOI: 10.1002/adom.202102169

(PEG) derivatives. The guest molecules are two luminophores benzene and naphthalene connected to the PEG chain through the ester bond, respectively. This system has the following advantages: 1) the introduction of carbonyl groups into the guest molecules can reinforce ISC, spin–orbit coupling and the formation of ordered structures of pseudopolyrotaxane could limit non-radiative relaxation and vibration of phosphors, which is conducive to the generation of p-RTP; 2) compared with other supramolecular RTP materials, those supramolecular pseudopolyrotaxane systems have the excitation-wavelength-responsive multicolor p-RTP emission at room temperature; 3) most importantly, the photochromic DAE can control the p-RTP emission of the system to realize a photoreversible afterglow switch. Therefore, the information storage and multilevel encryption can be achieved by utilizing multicolor display and photoreversibility of this supramolecular pseudopolyrotaxane system.

Herein, we prepared two kinds of PEG derivatives, i.e., BPEG and NPEG, based on benzene and naphthalene chromophores (**Scheme 1**). Two kinds of supramolecular pseudopolyrotaxanes, i.e., BPR and NPR, could be constructed via the host–guest interaction of PEG chain and $\alpha$-CD by simply adding a certain amount of PEG derivatives to the saturated $\alpha$-CD aqueous solution. 1H NMR of supramolecular pseudopolyrotaxanes showed that the number of $\alpha$-CD that thread on the PEG chain is about eight (Figures S5 and S6, Supporting Information). In the case of BPR, the number is calculated by comparing the H1 protons of $\alpha$-CD at 5.05 ppm (one $\alpha$-CD unit has 6 H1 protons) and the aromatic ring of BPEG at 8.20 ppm (a molecule of PEG chain has 4 benzene protons) is 7.48. For NPR, this number changes to 8.15. The rotating frame overhauser effect spectroscopy spectrum showed a clear ROE correlation between the protons of PEG and the interior protons of CD, demonstrating that the PEG chain was thread into CD cavity (Figures S7 and S8, Supporting Information). The powder X-ray diffraction analysis of BPR and NPR showed a strong reflection peak at $2\theta = 20.0°$ ($d$ = 4.44 Å) indicating the formation of a channel-type crystalline structure (Figure S9, Supporting Information).[20] Furthermore, scanning electron microscopy images (Figure S10, Supporting Information) of supramolecular pseudopolyrotaxanes showed a number of lamellar nanosheets with an average size of 500 nm. These results demonstrated that the host–guest interaction and the stacked structure of supramolecular pseudopolyrotaxane provide a protective environment to promote RTP emission.

## 2. Results and Discussion

In order to investigate the luminescence behaviors of BPR and NPR, a series of spectroscopic experiments were performed. The ultraviolet (UV) absorption and fluorescence spectra of the guest molecules in the aqueous solution were investigate. The fluorescence spectrum of BPEG exhibited a fluorescence emission at 324 nm (fluorescence lifetime = 0.82 ns, quantum yield = 1.61%) and the fluorescence spectrum of NPEG gave an emission at 372 nm (fluorescence lifetime = 15.22 ns) and 388 nm (fluorescence lifetime = 15.42 ns) with 54.47% quantum yield, respectively (Figures S11 and S12, Supporting Information). No phosphorescence emission was observed for BPEG or NPEG. Due to the poor water solubility, the luminescence behavior of BPR and NPR was investigated in the solid state. Upon 254 nm UV illumination, the solid powder of BPR or NPR glowed bright blue or greenish-yellow photoluminescence with long-lived phosphorescence and afterglow phenomenon that could be observed by the naked eye for ≈0.5 or 2 s after ceasing the UV light irradiation under ambient conditions (**Figure 1**a, Video S1, Supporting Information). In the

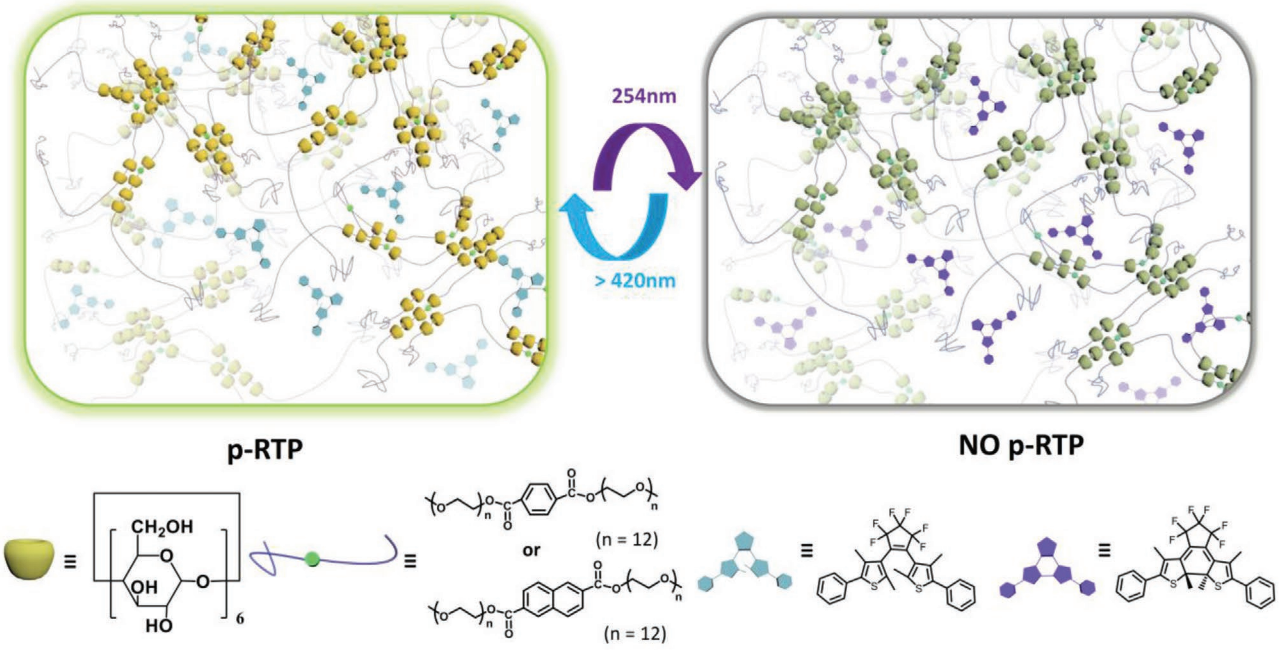

**Scheme 1.** Photoreversible multicolor p-RTP supramolecular pseudopolyrotaxanes.

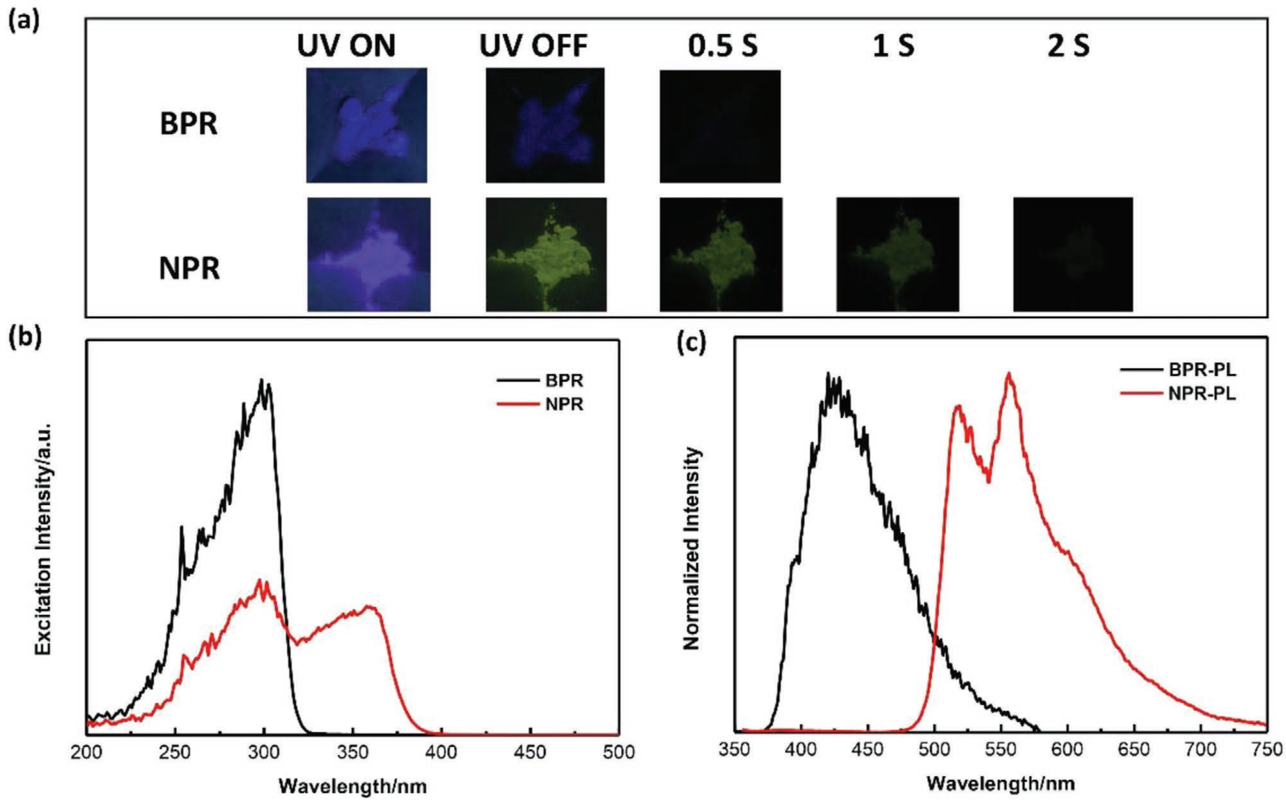

**Figure 1.** a) Photographs of BPR, NPR taken under 254 nm UV light and at different time intervals after ceasing irradiation. b) Phosphorescence excitation spectra and c) emission spectra measurements of BPR, NPR under ambient conditions excited at 300 nm.

phosphorescence excitation spectra and emission spectra measurements at room temperature (Figure 1b,c), the maximum excitation wavelength of BPR or NPR was 300 nm. When the excitation wavelength ranged from 225 to 325 nm, both BPR and NPR phosphorescence could be excited, but only NPR could be excited in the wavelength range of 325 to 400 nm. The phosphorescence emission spectra of BPR exhibited the emission bands peaking near 425 nm, and its phosphorescence lifetime and quantum yield were 57.94 ms and 0.39% respectively (Figure S13, Supporting Information). Significantly, NPR gave two phosphorescence emission bands at 517 and 556 nm at room temperature accompanied by the ultralong lifetimes up to 705.18 ms (556 nm) and 721.37 ms (517 nm) as well as a phosphorescence quantum yield of 3.67% (Figure S14, Supporting Information). These millisecond scale lifetimes are consistent with the characteristics of phosphorescence emissions. In addition, we further investigated the prompt and the delayed (0.1 ms) photoluminescence spectrum of BPR and NPR at different temperatures (Figures S15 and S16). The results showed that the prompt photoluminescence emission of BPR at 425 nm increased significantly when the temperature decreased from 297 to 77 K. Because the fluorescence emission in the prompt photoluminescence spectrum of NPR is dominant, and the influence of temperature on its phosphorescence emission cannot be got from the photoluminescence spectrum, we studied the delayed (0.1 ms) photoluminescence spectrum of NPR at different temperatures. The delayed photoluminescence emission of NPR at 556 nm also increased when the temperature decreased. It is well known that the low temperature can suppress the non-radiative relaxation process of the triplet state to the ground state ($S_0$) to promote phosphorescence enhancement. The above results demonstrate that the luminescence of BPR (at 425 nm) and NPR (at 556 nm) belong to the phosphorescence emission. The phosphorescence lifetime at low temperature further proves this phosphorescence characteristic (Figures S17 and S18, Supporting Information). Compared to 297 K, the lifetimes of BPR and NPR both increased at 77 K, and the phosphorescence intensity of NPR did not increase significantly when it changed from 297 to 77 K compared to that of BPR. This phenomenon is mainly due to the difference in the binding ability of $\alpha$-CD to chromophores. Compared with benzene ring, the binding ability of $\alpha$-CD to naphthalene ring is weaker.[21] Moreover, the inclusion of naphthalene and CD is enthalpy-driven. In this system, although low temperature promotes phosphorescence emission, the weaker inclusion of naphthalene chromophore and CD at low temperature disfavors the formation of assembly, which is also an important factor in promoting phosphorescence emission. Therefore, the effect of low temperature appears to be weaker for NPR.

It is documented that the chromophores with different degrees of conjugation may lead to the different p-RTP emission.[22] The fluorescence and RTP center of BPR and NPR is the carbonyl-containing benzene group and carbonyl-containing naphthalene group on the guest molecule, respectively. The phosphorescence emissions of pseudopolyrotaxane are basically consistent with these of the previously reported benzene and naphthalene derivatives.[16,23] According to the above experimental results, we speculated that the following factors mainly promoted the effective phosphorescence emission of the supramolecular system. Both BPEG and NPEG possess the ester bond, and the introduction of carbonyl groups can reinforce ISC and spin–orbit coupling for generating efficient phosphorescence emission.[23] On the other hand, the host molecule CDs can form channel-type crystalline structure pseudopolyrotaxane with the guest molecules through hydrogen bonding and hydrophobic interaction. The abundant hydrogen bonds in this ordered structure will suppress molecular vibration and non-radiative decay, thereby further promoting RTP emission. Meanwhile, the pseudopolyrotaxane structure can effectively avoid the side effects caused by the energy transfer and aggregation of chromophores. In the control experiment, the solid obtained by freeze-drying the solutions of adding BPEG or NPEG to D-glucopyranose showed no phosphorescence (Figure S19, Supporting Information). Such a control experiment demonstrates that the host–guest interaction is the key factor for the RTP of supramolecular assemblies.

In order to further explain the reason for the enhanced phosphorescence emission, we performed theoretical calculations of host-guest inclusion compound between model molecule bis(2-(2-methoxyethoxy)ethyl) naphthalene-2,6-dicarboxylate(MNp) and CD (see Supporting Information for details). The optimized structures of MNp$\subset$CD-$S_0$ and MNp$\subset$CD-$T_1$ are shown in Figure S20 (Supporting Information). The structures of the compound $S_0$ and the first-excited-triplet-state are similar greatly due to the interaction of hydrogen bonds. As can be seen in Figure S21 (Supporting Information), calculation results indicate that there are strong hydrogen-bonding interactions in the MNp$\subset$CD-$T_1$ complex. In Figure S21a (Supporting Information), O1 of guest molecule MNp and H3 of CD formed a hydrogen bond with the MNP-O1···H3-CD distance of 0.181 nm. The H4 of CD is presumably located at the center of one benzene ring of the guest molecule MNp, which indicates a strong C–H $\pi$ interaction between CD and the guest molecule MNp with the H4-benzene center distance of 0.268 nm. In Figure S21b (Supporting Information), O2 of guest molecule MNp and H5 of CD formed a hydrogen bond with the MNp-O2···H5-CD distance of 0.179 nm. The hydrogen bond forms between the guest molecule MNp and CD, resulting in a MNp-O3···H8-O4-CD distance of 0.185 nm and a bond angle of 172.5°, which is a strong hydrogen-bonding interaction. Guest molecule MNp and CD also have a certain steric effect, for example, there are multiple hydrogen bonds close to each other with the H1-H2 distance of 0.246 nm and the H6-H7 distance of 0.221 nm, which also limits the rotation of chemical bonds of guest molecules resulting in reducing energy dissipation. The hydrogen-bonding interactions between guest molecules MNp and CD make the rotation of single bonds of guest molecules MNp relatively difficult, which will decrease the energy dissipation of MNp$\subset$CD complex in the first-excited-triplet-state and enhance the phosphorescent emission. These calculation results indicate that the hydrogen bond on CD plays an important role in promoting the phosphorescence emission.

The photosensitizer is excited in the $S_0$ by absorbing light of a specific wavelength, which is transferred from $S_0$ to the first excited singlet state ($S_1$). Then, energy is transferred from its $S_1$ to the lowest excited triplet state ($T_1$) through the relaxation process of ISC. The ISC efficiency of the sensitizer is inversely proportional to the energy barrier value ($\Delta E_{st}$) which is the energy gap between the $S_1$ and $T_1$ states. As can be seen in Figure S22 (Supporting Information), the calculation result shows that, when the molecule contains carbonyl, $\Delta E_{st}$ = 20.2 kcal mol$^{-1}$, and when there is no carbonyl, $\Delta E_{st}$ = 28.0 kcal mol$^{-1}$. The results indicate that in the presence of carbonyl group, due to p-$\pi$ conjugation, the relaxation process of ISC is easier to occur. Then, the phosphorescent emission is enhanced. These calculated results confirm our speculation that the presence of carbonyl groups enhances the phosphorescence emission. According to theoretical and experimental results, we believe that BPR and NPR have similar mechanisms for enhancing phosphorescence emission by the synergistic effect of carbonyl groups, hydrogen bonds and host–guest interactions to promote ISC, limit molecular motion and reduce non-radiative decay.

Since BPR and NPR have different colors of phosphorescent emissions, we can reasonably speculate that the ratio variation of different luminophores may have a significant impact on the p-RTP color in the resulting supramolecular pseudopolyrotaxane. A series of multicomponent pseudopolyrotaxane with different molar feed ratio of BPEG/NPEG changed from 1:1, 2:1, 4:1, 5:1, 7:1, and 10:1 were prepared. As shown in phosphorescence emission spectra, with the increase of the molar feed ratio, the corresponding BPR phosphorescence intensity at 425 nm increases, accompanied by the decrease of NPR phosphorescence intensities at 517 and 556 nm (**Figure 2**b). This series of pseudopolyrotaxanes depicted various p-RTP colors from blue to greenish-yellow, lasting for up to 2 s by the naked eye after ceasing the 254 nm UV lamp irradiation (Figure 2a). The Commission Internationale de l'Éclairage (CIE) coordinates of multicomponent pseudopolyrotaxanes (Figure 2b) evolved from (0.16, 0.10) to (0.27, 0.32) and then to (0.39, 0.56), indicating that the color change matches well fits the naked-eye observation. More importantly, the supramolecular system displayed the time-dependent p-RTP property, presenting the different p-RTP colors of multicomponent pseudopolyrotaxanes with evolution at different time after ceasing the UV light irradiation (Figure 1a). Furthermore, these multicomponent pseudopolyrotaxane systems also have the excitation-wavelength-responsive afterglow emission (Figures S23 and S26, Supporting Information). Taking BNPR-5 as examples, when the excitation wavelength ranged from 260 to 360 nm, the phosphorescence emission spectra showed a difference in the intensity of the emission bands at 425 and 556 nm (Figure 2d). The coordinates on the corresponding CIE diagram also changed from the blue region to the greenish-yellow region, which was also in line with the observation by the naked eye. This property could be explained by the fact that the supramolecular system has two isolate phosphorescent emission species, i.e., BPR and NPR, with different excitations. According to their excitation spectra (Figures 1b and 2c), this series of pseudopolyrotaxanes can be excited with an excitation wavelength in the range of 225–400 nm. When the excitation wavelength is 260, 280, and 300 nm, two chromophores species jointly emit phosphorescence. Under the excitation of 320 and 340 nm, only the yellow-green phosphorescent emission of NPR can be excited. This time-dependent and excitation-wavelength-responsive

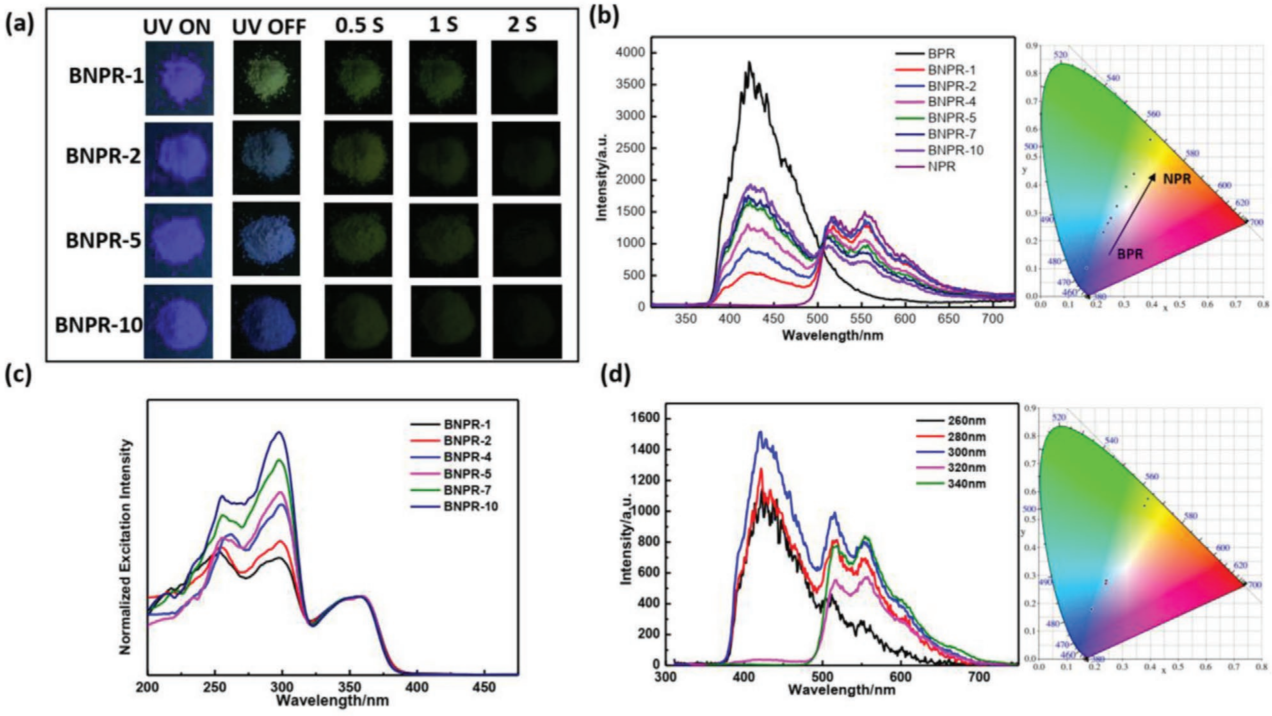

**Figure 2.** a) Photographs of the series of supramolecular pseudopolyrotaxane polymers taken under 254 nm UV light and at different time intervals after ceasing irradiation. b) Phosphorescence spectra and CIE chromaticity diagram of the series of supramolecular pseudopolyrotaxane polymers under ambient conditions excited at 300 nm. c) Normalized phosphorescence excitation spectra of the series of supramolecular pseudopolyrotaxane polymers under ambient conditions. d) Phosphorescence spectra and CIE chromaticity diagram of BNPR-5 with excitation varied from 260 to 340 nm under ambient conditions.

multicolor p-RTP feature of supramolecular pseudopolyrotaxanes endows them potential applications in the field of smart anti-counterfeiting materials.

DAE derivatives are promising building blocks for constructing photo-responsive supramolecular systems due to their outstanding photochromic properties.[24] Herein, 1,2-bis(2,4-dimethyl-5-phenyl-3-thienyl)-3,3,4,4,5,5-hexafluoro-1-cyclopentene was selected to provide the photoreversible switching function to the supramolecular pseudopolyrotaxane system (Figure S27, Supporting Information). The UV–vis absorption spectra of DAE indicated that it could interconverted between open and closed forms upon light irradiation (Figure S28, Supporting Information). With the irradiation of 254 nm UV light, the maximum absorption peak at 273 nm assigned to the open form DAE (OF-DAE) decreased, and the absorption peak at 571 nm assigned to the closed form of DAE (CF-DAE) was constantly rising. **Figure 3**a revealed that the phosphorescence emission of NPR and the UV absorption of CF-DAE had excellent spectral overlap. In contrast, there was no spectral overlap between NPR and OF-DAE. Therefore, we can speculate that the energy transfer could occur form NPR to CF-DAE, thereby quenching the phosphorescence of supramolecular pseudopolyrotaxane. In the photoreversible p-RTP system (NPR/DAE) composed of 91 wt% NPR and 9 wt% DAE, the greenish-yellow p-RTP was quenched by UV light (254 nm) irradiation (Figure S29, Supporting Information), while the quenched p-RTP function was recovered by irradiation with visible light (>420 nm). As shown in the photographs in Figure 3c and Video S2 (Supporting Information), the disappearance and recovery of afterglows could be observed by the naked eye. Figure 3b shows the phosphorescence spectra of photoreversible p-RTP system under alternate irradiation of UV light and visible light. A reasonable explanation of this property is as follows: The phosphorescence intensity at 556 nm decreased due to the formation of CF-DAE caused by UV radiation, which triggered the energy transfer between NPR and CF-DAE and thus led to the quenching of p-RTP from NPR. Subsequently, under UV irradiation, the conversion of CF-DAE to OF-DAE led to the interruption of energy transfer process, and the phosphorescence emission of the photoreversible p-RTP supramolecular system recovered at the same time. The changing behavior of phosphorescence intensity during alternating UV and vis irradiation illustrated that the conversion process of the photoreversible on-off p-RTP supramolecular pseudopolyrotaxane system could repeated for several times without obvious light fatigue (Figure 3d). All these results demonstrated that the p-RTP supramolecular polymer had excellent photoreversibility.

The fact that the p-RTP emission of supramolecular polyrotaxane can obviously respond to UV and vis light brings promising applications in the field of information storage and encryption. Morse code, as a language code, expresses different English letters, numbers, and punctuation marks through the sequence of dots (".") and dashes ("–"), and further conveys information. Inspired by the photo reversibility of the p-RTP system, an information storage and encryption medium based on supramolecular pseudopolyrotaxane to transmit information

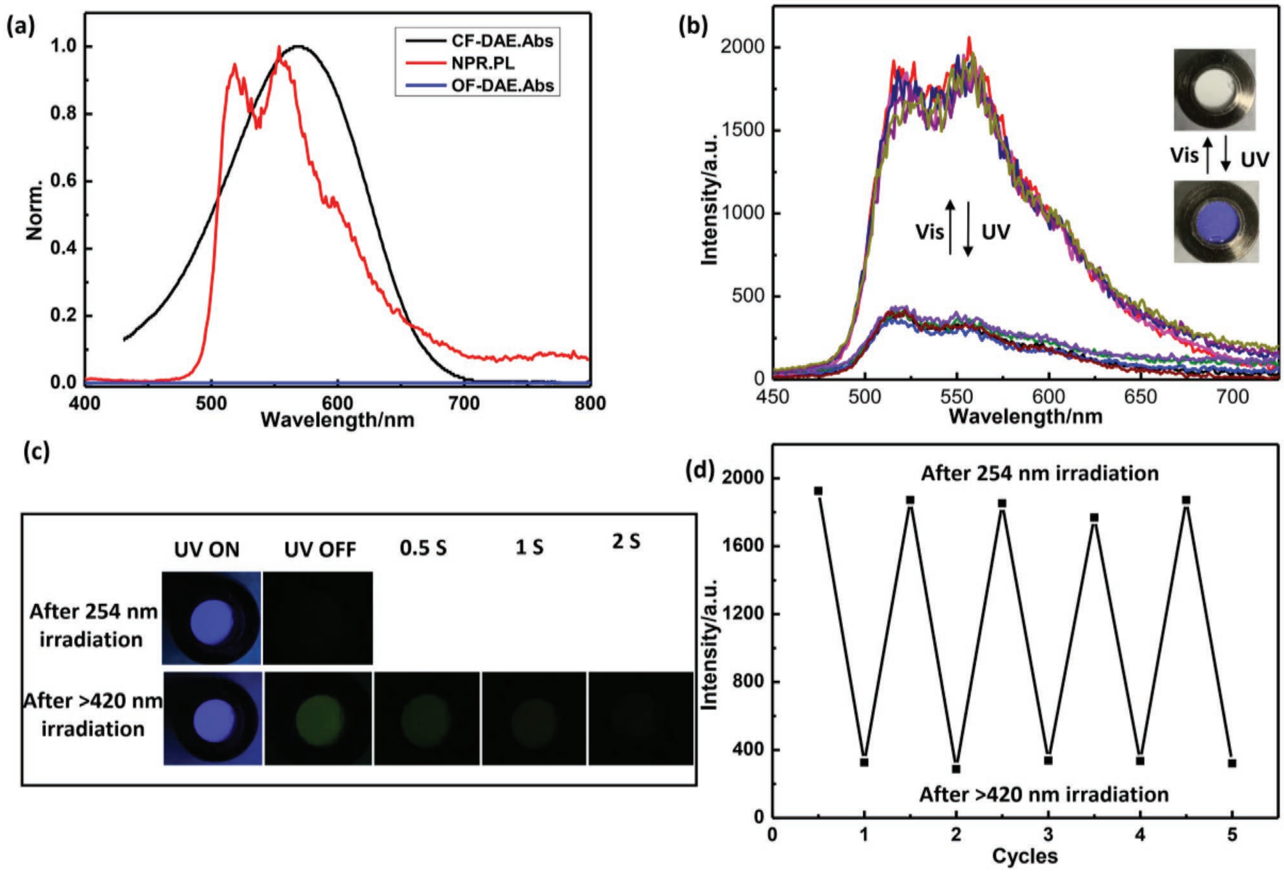

**Figure 3.** a) Normalized absorption spectrum of OF-DAE and CF-DAE in CHCl3 and phosphorescence emission spectrum of NPR in solid. b) Phosphorescence emission spectrum ($\lambda_{ex}$ = 300 nm) and (inset) photographs of NPR/DAE upon alternating UV (254 nm) irradiation for 10 min and Vis (>420 nm) irradiation for 3 min. c) Photographs of the photoswitching p-RTP under 254 nm UV light and at different time intervals after ceasing irradiation when the NPR/DAE are repeated by exposure to UV (254 nm) and Vis (>420 nm) light. d) Phosphorescence intensity change at 556 nm ($\lambda_{ex}$ = 300 nm) when the NPR/DAE are repeated by exposure to UV (254 nm) and Vis (>420 nm) light.

through Morse code had been developed. First, the p-RTP imaging is used for information storage. As shown in **Figure 4**a and Video S3 (Supporting Information), NPR/DAE was used as the recording medium. The p-RTP imaging was obtained by blocking UV light through a photo mask, and it could be erased by vis irradiation. In the initial state, the entire area of the recording medium had yellow-green p-RTP emission when the UV excitation was removed. Then, the medium was irradiated with 254 nm UV light for a period of time through a photomask, whose black part was opaque and showed the message "NKU" via the Morse code. The DAE of the supramolecular system in the illuminated part became a closed form to quench the p-RTP of NPR, and the p-RTP image representing the message "NKU" appeared and lasted for a few seconds after removing the 254 nm excitation. The recorded p-RTP image information can be erased by irradiating the entire sample with vis light (>420 nm) to restore it to original state. Benefitting from the photoreversible on–off switch p-RTP properties of the supramolecular system, this information storage material can be repeatedly reused. Then we used the different p-RTP characteristics of these pseudopolyrotaxane polymers to make time-resolved information encryption codes. The Morse code of the message "VJB" was prepared by arranging different polymer powders on paper, and different numbers represent the polymer at the corresponding position, as shown in Figure 4b and Video S4 (Supporting Information). Under the UV lamp of 254 nm, the solid powder emits blue fluorescence. When the excitation was turned off, the multi-color Morse code "VJB" showed due to the polymer emitting different p-RTP colors. Thereafter, the p-RTP emission of the position 1 was attenuated to be invisible and the color in other positions changed to yellow-green due to the short-lived luminescence of BPR species, and the remaining part showed the yellow-green message "SJB". When we continued to irradiate the Morse code with 254 nm UV lamp for ten minutes and then removed, the information displayed by the p-RTP of the pseudopolyrotaxanes system changed. In this case, the multi-color Morse code represented the message "VOS" appeared. Then the message "SOS", representing the international code signal of extreme distress, was displayed. The code evolved owing to the photoisomerization of DAE in the polymer at position 9. Therein, the excellent photoreversibility of DAE also gave the code change repeatability. Therefore, we realized visible, time-resolved multi-level information encryption by supramolecular polymers with different lifetimes. This research provides new ideas for the development of secure information storage and anti-counterfeiting.

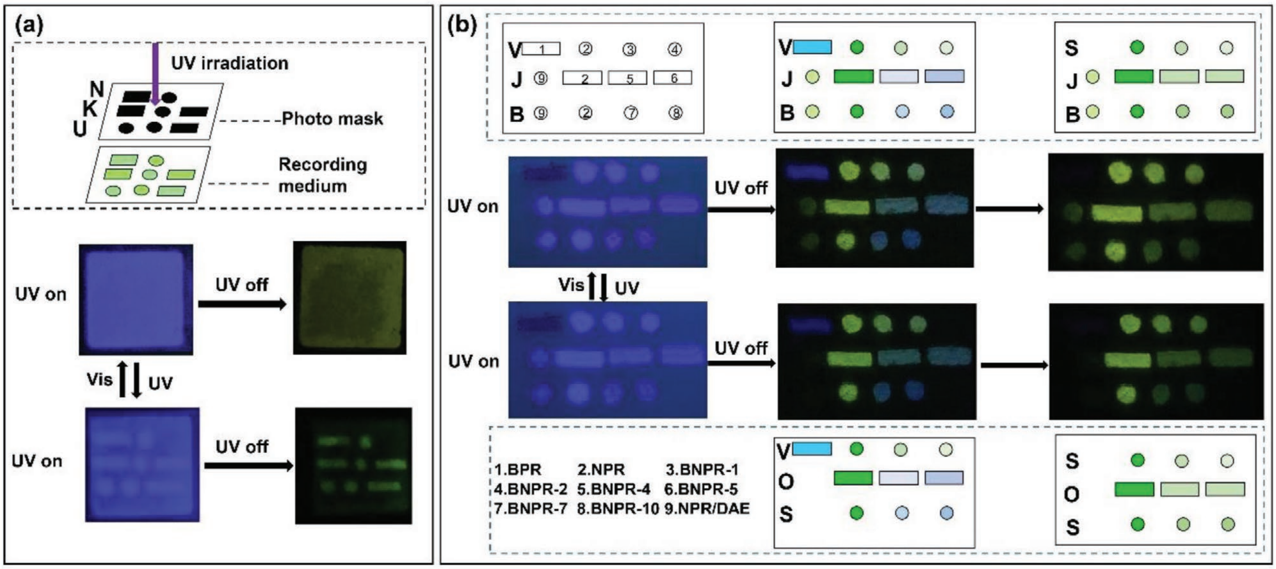

**Figure 4.** a) Illustration of the photoreversible p-RTP images for information storage. NPR/DAE as the recording medium. b) Time-resolved information encryption by a series of supramolecular pseudopolyrotaxane polymers.

## 3. Conclusion

In summary, we have proposed an effective and simple strategy to achieve p-RTP with color tunable and photoreversible switching properties in the supramolecular pseudopolyrotaxane polymer constructed by $\alpha$-CD and PEG derivatives of anthracene and naphthalene. The carbonyl groups, the abundant hydrogen bonds and the rigid channel-type crystalline structures of pseudopolyrotaxane in the system can reinforce ISC and inhibit luminophores vibration and non-radiative decay for promoting p-RTP emissions. The pseudorotaxanes formed by two different chromophores have different colors afterglows but comparable lifetimes, which endow the system with excitation-wavelength-responsive and time-dependent afterglow emission properties. Intriguingly, the photoreversible switching property of p-RTP in pseudopolyrotaxane materials composed of NPR and DAE was demonstrated. The p-RTP of NPR quenched after irradiation with UV lamp and recovered after vis light irradiation. The multicolor and photoreversible p-RTP features of supramolecular pseudopolyrotaxane polymers system can enrich the coding information of the pure organic materials for advanced time-resolved information encryption.

## Supporting Information

Supporting Information is available from the Wiley Online Library or from the author.

## Acknowledgements

This work was financially supported by NNSFC (Nos. 22131008 and 21971127).

## Conflict of Interest

The authors declare no conflict of interest.

## Data Availability Statement

The data that support the findings of this study are available in the supplementary material of this article.

## Keywords

cyclodextrin, photo-controlled, room-temperature phosphorescence, supramolecular pseudopolyrotaxane

Received: October 10, 2021
Revised: December 1, 2021

---

[1] a) J. Z. Zhao, W. H. Wu, J. F. Sun, S. Guo, *Chem. Soc. Rev.* **2013**, *42*, 5323; b) W. Zhou, Y. Chen, X. Dai, H. Y. Zhang, Y. Liu, *Org. Lett.* **2019**, *21*, 9363; c) X. K. Yu, W. T. Liang, Q. F. Huang, W. H. Wu, J. J. Chruma, C. Yang, *Chem. Commun.* **2019**, *55*, 3156; d) D. H. Dai, Z. Li, J. Yang, C. Y. Wang, J. R. Wu, Y. Wang, D. M. Zhang, Y.-W. Yang, *J. Am. Chem. Soc.* **2019**, *141*, 4756.

[2] a) M. S. Kwon, D. Lee, S. Seo, J. Jung, J. Kim, *Angew. Chem., Int. Ed.* **2014**, *53*, 11177; b) H. Chen, X. Y. Yao, X. Ma, H. Tian, *Adv. Opt. Mater.* **2016**, *4*, 1397; c) M. S. Kwon, Y. Yu, C. Coburn, A. W. Phillips, K. Chung, A. Shanker, J. Jung, G. Kim, K. Pipe, S. R. Forrest, J. H. Youk, J. Gierschner, J. Kim, *Nat. Commun.* **2015**, *6*, 8947; d) X. Dou, T. Zhu, Z. Wang, W. Sun, Y. Lai, K. Sui, Y. Tan, Y. Zhang, W. Z. Yuan, *Adv. Mater.* **2020**, *32*, 2004768; e) W. L. Zhou, W. J. Lin, Y. Chen, X. Y. Dai, Z. X. Liu, Y. Liu, *Chem. Sci.* **2021**, https://doi.org/10.1039/D1SC05861D.

[3] a) G. Zhang, G. M. Palmer, M. W. Dewhirst, C. L. Fraser, *Nat. Mater.* **2009**, *8*, 747; b) W. L. Zhou, Y. Chen, Q. Yu, H. Zhang, Z. X. Liu, X. Y. Dai, J. J. Li, Y. Liu, *Nat. Commun.* **2020**, *11*, 4655; c) D. A. Xu, Q. Y. Zhou, X. Y. Dai, X. K. Ma, Y. M. Zhang, X. F. Xu, Y. Liu, *Chin. Chem. Lett.* **2021**, https://doi.org/10.1016/j.cclet.2021.08.001.

[4] a) Q. W. Zhang, D. Li, X. Li, P. B. White, J. Mecinović, X. Ma, H. Ågren, R. J. M. Nolte, H. Tian, *J. Am. Chem. Soc.* **2016**, *138*, 13541; b) D. Li, F. Lu, J. Wang, W. Hu, X. M. Cao, X. Ma, H. Tian, *J. Am. Chem. Soc.* **2018**, *140*, 1916.

[5] Z. He, W. Zhao, J. W. Y. Lam, Q. Peng, H. Ma, G. Liang, Z. Shuai, B. Z. Tang, *Nat. Commun.* **2017**, *8*, 416.

[6] X. Liang, T. T. Liu, Z. P. Yan, Y. Zhou, J. Su, X. F. Luo, Z. G. Wu, Y. Wang, Y. X. Zheng, J. L. Zuo, *Angew. Chem., Int. Ed.* **2019**, *58*, 17220.

[7] H. Wu, L. Gu, G. V. Baryshnikov, H. Wang, B. F. Minaev, H. Agren, Y. Zhao, *ACS Appl. Mater. Interfaces* **2020**, *12*, 20765.

[8] Z.-Y. Zhang, W.-W. Xu, W.-S. Xu, J. Niu, X.-H. Sun, Y. Liu, *Angew. Chem., Int. Ed.* **2020**, *59*, 18748.

[9] a) F.-F. Shen, Y. Chen, X. Y. Dai, H.-Y. Zhang, B. Zhang, Y. H. Liu, Y. Liu, *Chem. Sci.* **2021**, *12*, 1851; b) J.-J. Li, H.-Y. Zhang, Y. Zhang, W.-L. Zhou, Y. Liu, *Adv. Opt. Mater.* **2019**, *7*, 1900589.

[10] Z.-Y. Zhang, Y. Chen, Y. Liu, *Angew. Chem., Int. Ed.* **2019**, *58*, 6028.

[11] Z. Y. Zhang, Y. Liu, *Chem. Sci.* **2019**, *10*, 7773.

[12] X. K. Ma, W. Zhang, Z. Liu, H. Zhang, B. Zhang, Y. Liu, *Adv. Mater.* **2021**, *33*, 2007476.

[13] X. Yao, J. Wang, D. Jiao, Z. Huang, O. Mhirsi, F. Lossada, L. Chen, B. Haehnle, A. J. C. Kuehne, X. Ma, H. Tian, A. Walther, *Adv. Mater.* **2021**, *33*, 2005973.

[14] a) Y. Gong, G. Chen, Q. Peng, W. Z. Yuan, Y. Xie, S. Li, Y. Zhang, B. Z. Tang, *Adv. Mater.* **2015**, *27*, 6195; b) Y. Zhang, Y. Liu, *Chin. J. Org. Chem.* **2020**, *40*, 3802; c) M. Hao, G. P. Sun, M. Z. Zuo, Z. Q. Xu, Y. Chen, X.-Y. Hu, L. Y. Wang, *Angew. Chem., Int. Ed.* **2020**, *59*, 10095.

[15] C. Y. Li, X. Tang, L. Q. Zhang, C. H. Li, Z. P. Liu, Z. S. Bo, Y. Q. Dong, Y.-H. Tian, Y. P. Dong, B. Z. Tang, *Adv. Opt. Mater.* **2015**, *3*, 1184.

[16] X. Ma, C. Xu, J. Wang, H. Tian, *Angew. Chem., Int. Ed.* **2018**, *57*, 10854.

[17] a) H. Chen, L. Xu, X. Ma, H. Tian, *Polym. Chem.* **2016**, *7*, 3989; b) X. Ma, J. Cao, Q. Wang, H. Tian, *Chem. Commun.* **2011**, *47*, 3559; c) J. B. Yao, W. H. Wu, C. Xiao, D. Su, Z. H. Zhong, T. Mori, C. Yang, *Nat. Commun.* **2021**, *12*, 2600.

[18] Q.-W. Zhang, D. F. Li, X. Li, P. B. White, J. Mecinović, X. Ma, H. Ågren, R. J. M. Nolte, H. Tian, *J. Am. Chem. Soc.* **2016**, *138*, 13541.

[19] H. Chen, X. Ma, S. Wu, H. Tian, *Angew. Chem., Int. Ed.* **2014**, *53*, 14149.

[20] K. M. Huh, T. Ooya, S. Sasaki, N. Yui, *Macromolecules* **2001**, *34*, 2402.

[21] W. Saenger, *Angew. Chem., Int. Ed.* **1980**, *19*, 344.

[22] X. Y. Dou, T. W. Zhu, Z. S. Wang, W. Sun, Y. Y. Lai, K. Y. Sui, Y. Q. Tan, Y. M. Zhang, W. Z. Yuan, *Adv. Mater.* **2020**, *32*, 2004768.

[23] L. Gu, H. Wu, H. Ma, W. Ye, W. Jia, H. Wang, H. Chen, N. Zhang, D. Wang, C. Qian, Z. An, W. Huang, Y. L. Zhao, *Nat. Commun.* **2020**, *11*, 944.

[24] H. Wu, Y. Chen, X. Y. Dai, P. Y. Li, J. F. Stoddart, Y. Liu, *J. Am. Chem. Soc.* **2019**, *141*, 6583.